Experimental Thermal and Fluid Science 42 (2012) 38–45

Contents lists available at SciVerse ScienceDirect

Experimental Thermal and Fluid Science

journal homepage: www.elsevier.com/locate/etfs

Heat transfer enhancement by spinodal decomposition in micro heat exchangers

Stefano Farisè, Andrea Franzoni, Pietro Poesio *, Gian Paolo Beretta

Università degli Studi di Brescia, Dipartimento di Ingegneria Meccanica e Industriale, Via Branze 38, 25123 Brescia, Italy

ARTICLE INFO

Article history:
Received 12 December 2011
Received in revised form 26 March 2012
Accepted 27 March 2012
Available online 18 May 2012

Keywords:
Spinodal decomposition
Microdevice
Microcooling

ABSTRACT

In this work, we investigate experimentally how the heat transfer in a laminar flow can be enhanced by using a partially miscible binary liquid–liquid mixture undergoing spinodal decomposition. A mixture of acetone–hexadecane is quenched in a micro heat exchanger to induce spinodal decomposition. The heat transfer rate is enhanced by self-induced convective effects sustained by the free energy liberated during phase separation. We report a heat-transfer augmentation of up to 150% when phase separation occurs in microchannels. Since acetone and hexadecane are immiscible below a critical temperature of 27 °C, to obtain their spinodal decomposition the mixture inlet temperature are above 27 °C and the heat exchangers wall are well below. We measure the heat transfer with a feedback method instead of a direct measure. To validate this measuring technique we carefully verify the energy balance. We fabricated a copper single-channel heat sink and two different types of multi-channel array. The single-channel exchanger allows us to visualize the induced convection. The arrays of microchannels promise to achieve very high heat transfer coefficients with small flow rate.

1. Introduction

With the constant rush for miniaturization, especially in electronics, and the more widespread use of integrated systems, we need technologies that allow to exchange a large amount of heat in small devices and with the highest possible efficiency.

Tuckerman and Pease [1] first introduced the concept of microchannel heat sink, and since then several technologies have been developed to exchange heat more effectively.

An important distinction must be made between technologies that use a single-phase flow and those that use multiphase flows. Among the latter another distinction is between multiphase flows of a single constituent and flows of non-miscible phases.

Tuckerman and Pease [1] optimized the dimensions of the channels in terms of width and height for single-phase flow of water under the constraint of maximum allowable pressure drop and substrate surface temperature. They found that single-phase water-cooling could remove up to 790 W/cm^2. A similar optimization process was done by Upadhye and Kandlikar [2]. The main problem with single-phase flow heat transfer in microchannels is the low Nusselt number obtained in laminar flow – Shah and London [3] – of the order of 4.

Performance rises significantly using multi-phase technology. The study of boiling flows in a microchannel leads to much higher heat transfer coefficients due to the high heat of vaporization. Mudawar and Bowers [4], Mudawar [5] and Kandlikar [6] showed that flow boiling can remove up to 10,000 W/cm^2. While flow boiling is attractive because it delivers high heat flux at the constant temperature of the phase change, it can be difficult to control due to back flow, instabilities, and local dry-out – Kandlikar [7]. Usually water is the working fluid, but the problem is that the saturation temperature is higher than the operating temperature of most electronics. The proposed solution is to use refrigerants, instead of water, as working fluids since their boiling temperature is lower. Refrigerants, however, offer lower cooling capabilities due to a lower specific heat and heat of vaporization.

Wang et al. [8], to increase the Reynolds number, proposed the adoption of small nozzles that spray water on the surface to cool. Jet array helps to achieve uniform cooling of the chip surface where as a carefully located single jet can provide highly localized cooling of hot spots on chips with nonuniform heat generation.

Betz and Attinger [9] investigated segmented flow as a way to enhance single-phase heat transfer with water in microchannels. Segmented flow is a periodic pattern of non-condensable bubbles and liquid slugs created by a T-junction with the injection of air in liquid-filled microchannels. Experiments and optimization studies have demonstrated that segmented flow could enhance heat transfer by up to 40% in a microchannel heat sink, in comparison with single-phase flow at the same liquid flow rate. The increase in performance is significant, but the system requires the simultaneous use of both water and compressed air. This complicates the design of the heat exchanger and the tuning of the flow rate to keep the system stable and optimized.

In this paper we introduce the possibility of using spinodal mixtures to generate an evenly distributed microagitation which

* Corresponding author.
E-mail address: pietro.poesio@ing.unibs.it (P. Poesio).

0894-1777/$ - see front matter © 2012 Elsevier Inc. All rights reserved.
http://dx.doi.org/10.1016/j.expthermflusci.2012.03.024

increases the effective diffusivity that therefore increases the heat exchange. There are, in our opinion, several appealing features that motivate the use of spinodal mixtures for heat exchange purposes. The wide variety of bi and tri component spinodal mixtures allows one to find the critical temperature closer to the design parameters of the device to be cooled. Moreover, since the mixture remains liquid, there are no instabilities in the flow and no pumping problems. There is also no need to re-condense the gaseous phase. The composition of the mixture phases changes constantly with the variation in temperature so it is possible to obtain stirring at small scale by controlling where new domains form and grow by coalescence.

2. Theory

Spinodal decomposition is the spontaneous process whereby an unstable partially miscible liquid mixture relaxes toward a lower free energy (stable) equilibrium state. During this process, an initially homogeneous liquid solution of a given composition spontaneously changes from an unstable single-phase to a two-phase stable state consisting of two separated liquid phases, of different compositions, in mutual equilibrium. This is possible only if the overall Gibbs free energy of the two separated phases is lower than that of the initial single-phase mixture. When an initially homogeneous liquid mixture at high temperature is cooled rapidly across the coexistence (binodal) curve into the two-phase region, it undergoes phase segregation (demixing) either by nucleation or by spinodal decomposition. Nucleation occurs when quenching takes the system in a metastable equilibrium state (between the binodal and the spinodal curve): it is an activated process and a free energy barrier must be overcome in order to form critical nuclei that later grow and coalesce. Spinodal decomposition, instead, occurs spontaneously, without an energy barrier to overcome (the initial state is below the spinodal curve): all the concentration fluctuations are amplified regardless of their size and wavelength. If the mechanism of segregation is convection dominated, as occurs for low viscosity systems, drops move against each others under the influence of non-equilibrium capillary forces, the so-called Korteweg stresses Poesio et al. [10]. Recently, it has been shown that this self-induced disordered bulk flow can be used to increase the heat transfer rate both in a closed configuration Poesio et al. [11] and in small pipe flow Gat et al. [12] and Di Fede et al. [13]. Also numerical simulations predict a significant increase in heat transfer – Molin and Mauri [14].

3. Experimental setup

We have used an 'UCST' (upper critical solution temperature) bi-component system made by a mixture of acetone and hexadecane (i.e., there is a critical temperature above which the components are miscible in all proportions). This mixture has been selected because it is isopycnic, i.e., the two phases have almost the same density and, therefore, buoyancy effects are negligible. The components are also non-toxic and can be safely used in relatively large volumes. The excess volume of this mixture has been considered negligible as it is lower than 5%. The minimal complete miscibility temperature as shown in Fig. 1 is 27 °C and it is obtained using equal volume parts of the two components (y_{acn} = 0.799 in mole fraction of acetone).

Experimental data on the binodal curve are from Machedo and Rasmussen [15]. The spinodal curve is estimated using a two-parameter Margules-type model (Di Fede et al. [13]. To measure the heat transfer enhancement effect due to spinodal decomposition, we have developed a closed-loop experimental set-up (Fig. 2) that allows us to pump the mixture from a hot thermostatic

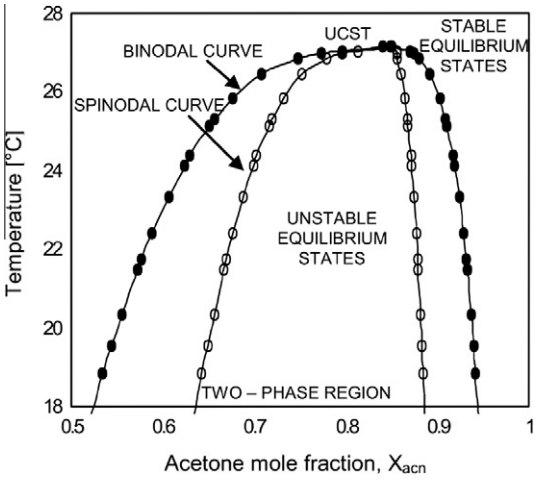

Fig. 1. Miscibility-gap phase diagram for acetone–hexadecane mixtures.

reservoir to the experimental test section where is quenched by the bold pipe walls.

The test section consists of a microheat exchanger. A Peltier cell is used to set and maintain the temperature of the cold side of the exchanger throughout the test. The temperature of the cold side of the Peltier cell is kept constant by a computer controlled PID (Proportional Integral Derivative controller) (which regulates the duty cycle of the electric power supplied to the cell to keep the temperature constant). A thermostatic bath is used to cool the hot side of the cell. With these devices the temperature on the cold side of the Peltier cell can be kept in a range of ±0.08 °C around the temperature set by the PC. Since we used this technique (that requires electric power and some sort of cooling) and not a second fluid to cool the mixture, we have no information about the actual amount of heat exchanged. We also need a controlled temperature at the inlet of the heat exchanger that must be above 27 °C. So we built and used a second heating thermostat, also controlled by the PC and agitated with a magnetic stirrer, to keep the temperature as uniform as possible and to facilitate the mixing of the mixture. The inlet temperature imposed to the fluid was measured in an interval of ±0.05 °C around the value set by the PC.

By reading the value of the duty cycle set by the PID feedback control we can estimate how much heat the hot thermostatic bath gives to the mixture reservoir to keep the temperature constant for the imposed conditions of cooling temperature and flow rate. We can, therefore, determine how much heat has been subtracted from the hot flow in the test section. Details of the simple calculation and validation of the technique are given in Sections 5.1 and 5.2. With this procedure we introduce a smaller uncertainty than measuring the heat given to an hypothetical cold flow because we do not need to know the properties of the fluid, the flow rate and the position of the thermocouples. Our measurement uncertainties are only due to the voltage applied to the resistor and to the value of resistance, and we are able to measure these quantities with an accuracy far greater than temperature and flow rate.

Our experiment has been done on three different types of heat exchangers.

The first and most simple is the single channel (Fig. 3A): we cut a channel (section of 0.7 × 0.7 mm and 38 mm long) in a piece of copper. The top and the bottom of the channel are sealed with a thin glass to record with a high-speed camera the test section. We placed a Peltier cell on each side of the channel to finely control the temperature and to be sure to have no gradient at all. A gradient would perturb the flow of the mixture and complicate the mechanics of heat transfer.

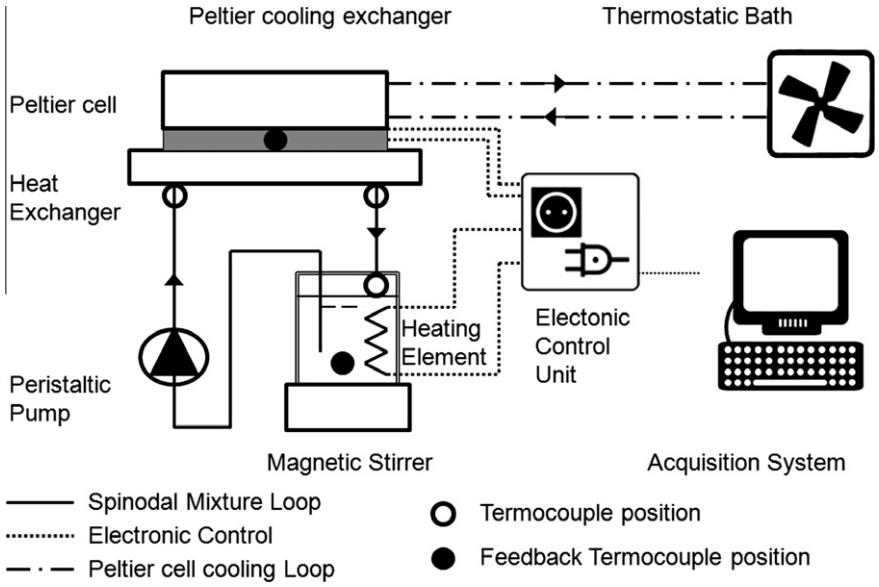

Fig. 2. Sketch of the experimental set-up.

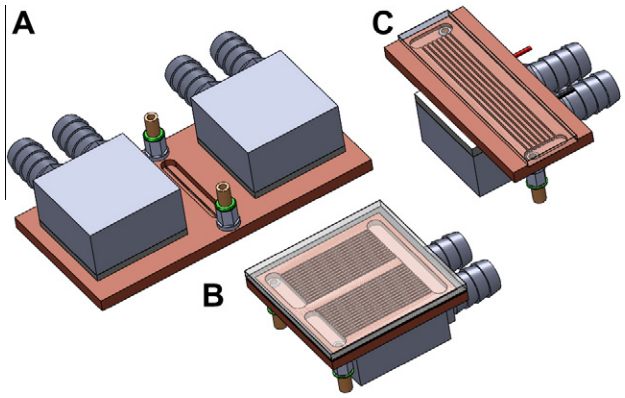

Fig. 3. The three heat exchangers we tested in our experimental setup.

We used this heat exchanger for visualization and validation purposes: the exchange area is small so the difference in heat exchange is small, too. Therefore, the experimental uncertainty is greater than that obtained using the other heat exchangers.

Despite the single channel is very useful to understand the mechanism of the spinodal decomposition, its industrial applications are limited. We have built a second heat exchanger with nine parallel channels (0.7×1.5 mm tall and 72 mm long). As the previous one this also has a glass top to view the flow pattern of the mixture during cooling. This set-up requires just a single Peltier cell placed behind the array of channels as shown in (Fig. 3B).

The third heat exchanger (Fig. 3C) is something very similar to the real heat sinks used to cool CPU's on PC's motherboards. It is a compact multi-channel array (14 channel) with a U shape. This too is sealed with a glass and cooled with a Peltier cell behind the channels.

We used a total of 5 (6 in the single channel configuration) thermocouples: the first is placed in the mixture reservoir to constantly monitor the temperature of the hot mixture and as a feedback for the PID controller of the hot thermostatic bath; the second and the third are placed at the inlet and at the outlet of the heat exchanger; the forth is placed at the end of the outflow hose just before the hot reservoir to verify the heat balance; the last one (or the last two in the single channel set-up) is placed on the cold side of the Peltier cell to set and monitor the cold side temperature and as a feedback for the Peltier cell PID controller.

All thermocouples are type T, fabricated in our lab by wires coming from the same hank; each thermocouple is calibrated using a cold bath (0 °C, ice/water), we could verify the resulting uncertainty to be in the range of ±0.2 °C. In addition, each measure presented in this paper has been obtained using the thermocouples differentially so that the uncertainty of measurement is reduced to ±0.08 °C.

In the following text we will only indicate the temperatures of the heated thermostatic reservoir and the cold side of the heat exchanger. Since the loop outside of the exchanger is very short and well insulated and the exchange area of the heat exchanger is relatively large, the temperatures of the inlet and the outlet of the test section (at least when the flow rate is greater than 10 Nl/min as we explain in Section 5.2) coincide with the temperatures of the heated reservoir and the cold side of the heat exchanger.

4. Experimental procedure

For each heat exchanger, tests were carried out with bi-distilled water (for validation purpose), pure acetone, pure hexadecane, and the spinodal mixture. The procedure is as follows:

- we switch on the thermostatic bath to cool the Peltier cell;
- we use the maximum flow rate available (30 ml/min) to ensure the best filling of the channels array;
- the flow rate is reduced to 10% of the maximum (3 ml/min);
- the temperature of the Peltier cell is brought to the desired value for the run;
- keeping fixed the temperature of the Peltier cell the heated reservoir temperature is increased to the desired value;
- we wait 5 min to reach a stable temperature condition and than we start the data acquisition;
- data for each flow rate are acquired for 5 min, then the flow rate is increased by 5%;
- the previous step is repeated until the maximum flow rate achievable in the test facility is reached;
- the temperature of the cold side of the heat exchanger is reduced and all the steps are repeated for the new temperature;
- the system is cleaned with solvent and dried with an air flow until complete drying.

The previous steps are repeated for each of the four fluids used in each heat exchanger.

5. Set-up validation

5.1. Heated reservoir maximum power

The first parameter that we need to know during the validation of our system is the maximum electric power converted via Joule effect into heat power by the resistance of the heated reservoir. We need to know this exact value because we do not record step by step the electrical power value but only the duty cycle value, DC(t), from which we estimate the converted power:

$$\dot{Q}_{el}(t) = \mathrm{DC}(t)\dot{Q}_{el}^{\mathrm{Max}}. \quad (1)$$

To evaluate this value we recorded a test section with the peristaltic pump off. By doing so and assuming that all the electrical power is converted into the heated bath, we can compute its value with this formula:

$$\dot{Q}_{el}^{\mathrm{Max}} = mc_p \frac{\mathrm{d}T}{\mathrm{d}t}. \quad (2)$$

Fig. 4 shows the trend of the temperature of the hot thermostatic bath during the test. It increases, as expected, almost linearly with time because the properties of water in this temperature range are, to a good approximation, constant. We used 200 ml of bi-distilled water and the frequency of the acquisition was 3 Hz.

5.2. Power balance validation

As already explained, to measure the heat transfer in the test section we measure the electrical power sent to the resistor in the magnetically stirred thermostat.

This technique avoids the need to have precise estimates of the temperature-dependent thermo-physical properties of the mixture and which we know from Di Fede et al. [13] are not known with good precision as function of the temperature.

Our technique relies on the fact that all the electrical power converted to heat by the resistor in the hot thermostat is exchanged across the test section. To demonstrate this fact, we write the power balance for our closed system as follows

$$\dot{Q}^{\rightarrow}_{\text{inlet pipe}} + \dot{Q}^{\rightarrow}_{\text{test section}} + \dot{Q}^{\rightarrow}_{\text{outlet pipe}} = \dot{Q}^{\leftarrow}_{\text{Joule}}, \quad (3)$$

$\dot{Q}^{\rightarrow}_{\text{inlet pipe}}$ is the heat lost by the inlet pipe between the hot thermostat and the test section; $\dot{Q}^{\rightarrow}_{\text{test section}}$ is the heat exchanged in the test section; $\dot{Q}^{\rightarrow}_{\text{outlet pipe}}$ is the heat exchanged in the outlet pipe, between the test section and the hot thermostat; and $\dot{Q}^{\leftarrow}_{\text{Joule}}$ is the electrical power converted to heat by the resistor in the hot thermostat.

Fig. 5 shows the various contributions for the U-shaped multichannel heat exchanger with water, T_{bath} = 35 °C and T_{Cu} = 25 °C.

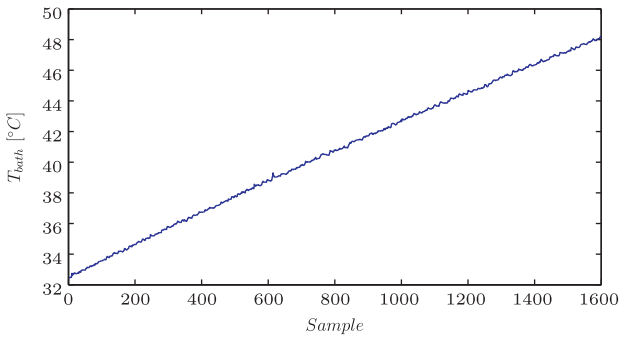

Fig. 4. T_{bath} versus time during the validation test to determine $\dot{Q}_{el}^{\mathrm{Max}}$.

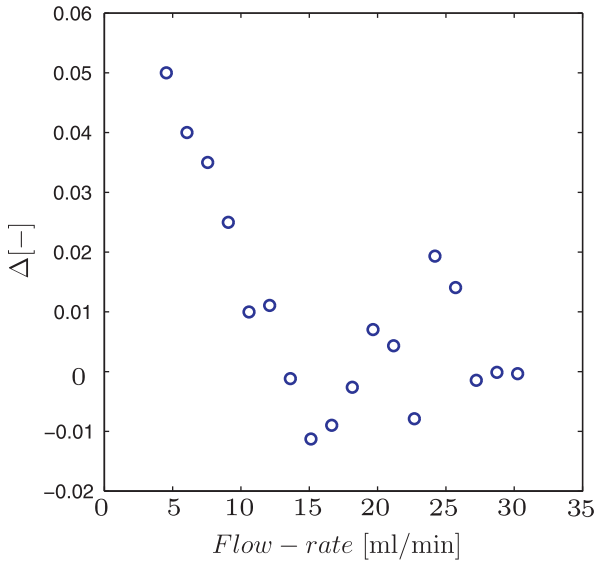

Fig. 5. Percentage difference $\Delta = (\dot{Q}_{\text{Joule}} - \dot{Q}_{\text{test section}} - \dot{Q}_{\text{inlet pipe}} - \dot{Q}_{\text{outlet pipe}})/\dot{Q}_{\text{Joule}}$.

It shows that the difference between the supplied electrical power and the heat exchanged in the test section and in the inlet and outlet pipes is always within a 5%. It is possible to see that the error is greater for the lower fluid velocities for two main reasons: (1) the heat exchanged is smaller so the percentage error is greater and (2) it is caused by the imperfect insulation of the hot reservoir. The contribution of $Q_{\text{inlet pipe}}$ and $Q_{\text{outlet pipe}}$ is always less than 1 W and almost constant during all tests. For this reason, we prefer to trust the data above 10 ml/min, but we will report all available data for the sake of completeness. After validating our system using water (it is the most stable fluid in the temperature range involved) we checked our assumption with the other pure fluids.

We use the measured temperatures of the mixture at inlet and outlet of the test section only to calculate the Nusselt number according to Eq. (4) below. For all subsequent correlations we use the value of Q_{Joule} derived from the feedback control of the heated reservoir.

5.3. Single channel heat exchanger validation

The single-channel exchanger is useful for our analysis because the theory behind the heat transfer in a square channel is well known, so comparing our results with the theoretical ones, we obtain a good feedback about the accuracy of our work.

The main problem we had in the data evaluation is the correct estimation of the inner exchange area of the channel. Due to geometry and sealing problems we could not put the thermocouples at the actual input and output of the channel, but we put them just outside the heat exchanger. This implies that the measured temperatures are not referred to the channel ends, but to the exchanger ones. Thus, the exchange area is greater that the channel area. Being difficult to measure directly, we measured the actual exchange area via software by using a 3D model.

The experimental data are consistent with the area measured this way, therefore, we used it for all subsequent calculations (see Fig. 6).

Fig. 7 shows the results for the Nusselt number, the points refer to the experimental data, while the line refers to the theoretical correlation. The Nusselt number is defined as:

$$\mathrm{Nu} = \frac{\dot{m}c_p\Delta T_{\text{measured}}}{A \cdot \Delta T_{\text{ml}}}\frac{L}{k} \quad (4)$$

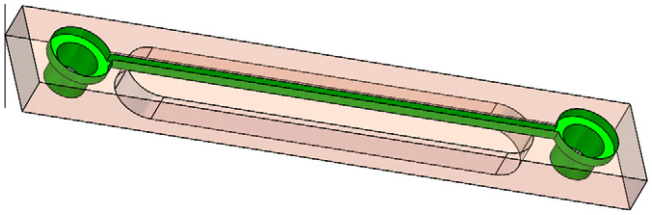

Fig. 6. Total exchange area in our microchannel heat exchanger.

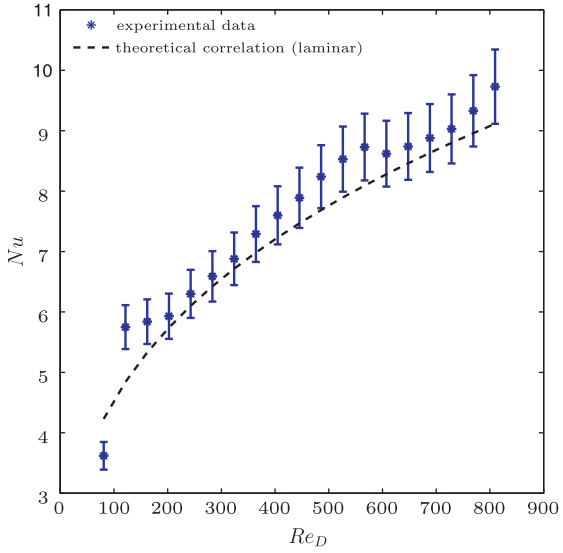

Fig. 7. Comparison between theoretical and experimental Nusselt numbers in a single-channel test with water, T_{bath} = 35 °C and T_{Cu} = 20 °C.

where $\Delta T_{\text{measured}}$ is the measured difference in temperature between inlet and outlet of the test section, ΔT_{ml} is the log-mean temperature difference between the mixture and the heat exchanger wall at inlet and outlet, $\dot{m}$ is the measured mass flow rate, L is the hydraulic diameter of the test section, k the thermal conductivity of the mixture, c_p the specific heat, A the test-section heat-exchange area.

6. Experimental results

To obtain the heat exchanged during phase transition, several experiments were conducted following the experimental procedure outlined in Section 4. The experimental results correspond to various flow rates of the solvent system in the heat exchangers at different inlet temperatures and wall temperatures. The experiments were conducted with pure fluids and with a mixture of critical composition (critical molar composition is $y_c = 0.799$ where $y = y_{acn}$ is the mole fraction of acetone and, of course, $1 - y = y_{hex}$ that of hexadecane) and with pure fluids.

6.1. Single channel heat exchanger

Figs. 8 and 9 show the results for the Nusselt number for pure acetone and pure hexadecane, respectively. The points refer to the experimental data, while the line refers to the theoretical correlation.

Even if the Reynolds numbers are always lower than the critical value for the laminar to turbulent transition, we see that the correlation for laminar flows does not work well. This is probably due to the inlet and the outlet hoses being perpendicular to the channel,

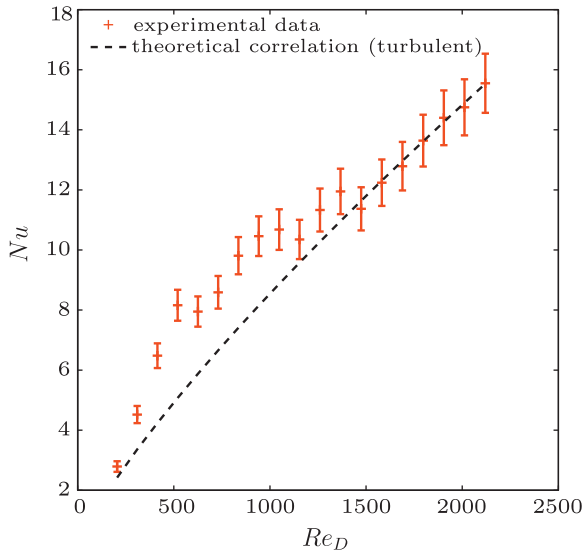

Fig. 8. Comparison between theoretical and experimental Nusselt numbers in a single-channel with pure acetone with T_{bath} = 35 °C and T_{Cu} = 20 °C.

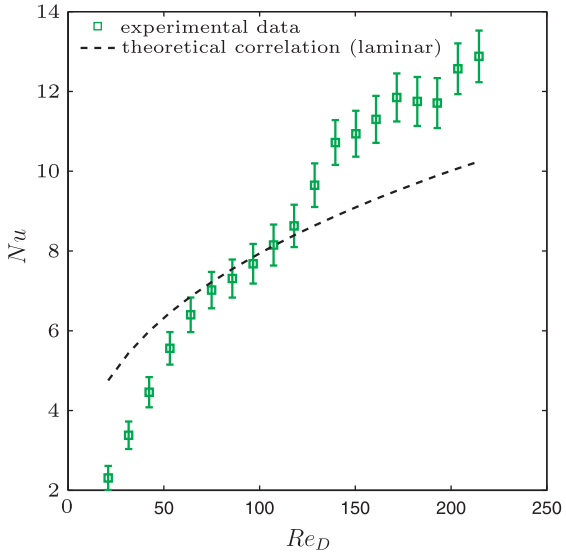

Fig. 9. Comparison between theoretical and experimental Nusselt numbers in a single-channel with pure hexadecane with T_{bath} = 35 °C and T_{Cu} = 20 °C.

causing an instability in the first part of the channel which maybe changes the motion from the expected laminar condition. The effect seems more pronounced for acetone (Fig. 8) than for water (Fig. 7). For water we find reasonable agreement with the laminar Stephan correlation for simultaneously developing laminar flow at constant wall temperature (Stephan and Preuer [16]). $\text{Nu} = 3.657 + \frac{0.0677((D/L)\text{Re}_D\text{Pr})^{4/3}}{1+0.01[(D/L)\text{Re}_D\text{Pr}]^{\frac{1}{3}}}$. For acetone the agreement is reasonable only if we compare with the turbulent Petukhov–Gnielinski correlation proposed in Gnielinski [17] $\text{Nu}_D = \frac{(f/8)(\text{Re}_D-1000)\text{Pr}}{1.00+12.7(f/8)^{1/2}(\text{Pr}^{2/3}-1)}$. This correlation is good for $0.5 < \text{Pr} < 2000$ and $3000 < \text{Re}_D < 5 \times 10^6$ where for smooth pipes, one should use the following for the friction factor: $f = (0.790\ln\text{Re}_D - 1.64)^{-2}$. For the single channel, L = 38 mm, D = 0.7 mm. Notice the difference in Prandtl number, respectively, 6.99, 3.60, 37.02, and 19.36 for water, acetone, hexadecane, and the critical mixture. As we can see from Fig. 9 hexadecane is probably in the laminar-to-turbolent transition regime

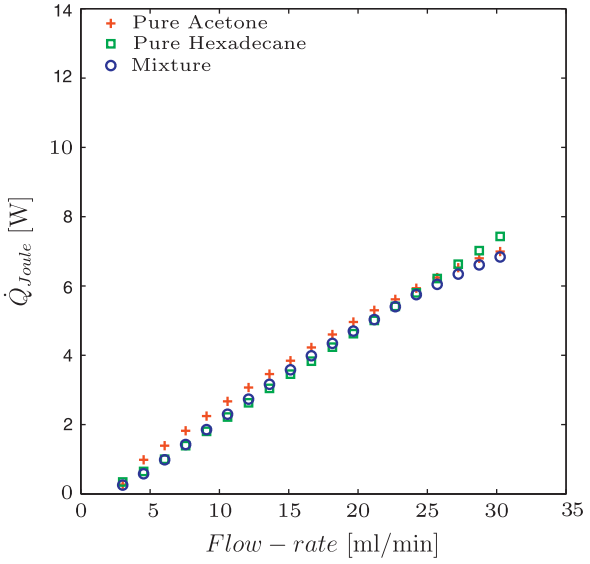

Fig. 10. Absorbed electrical power versus flow-rate with T_{bath} = 35 °C and T_{Cu} = 25 °C, measured for single channel flow of pure acetone, pure hexadecane, and a mixture of acetone and hexadecane with critical mole fraction (y_{acn} = 0.799). Mixture data and pure-component data show no important difference since spinodal decomposition occurs mildish for T_{Cu} = 25 °C.

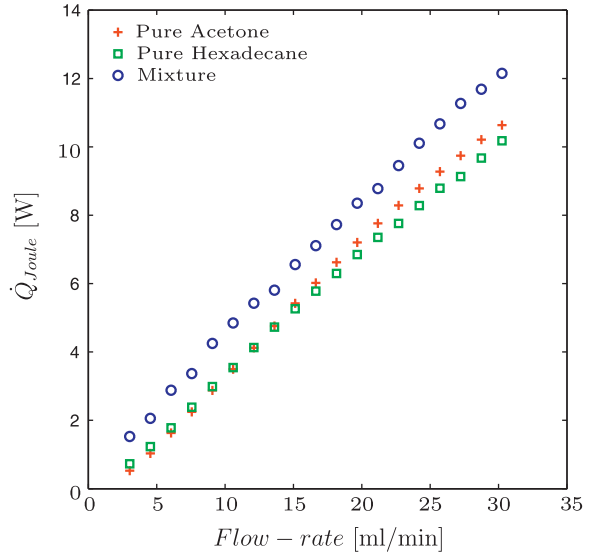

Fig. 12. Absorbed electrical power versus flow rate measured for single channel flow with T_{bath} = 35 °C and T_{Cu} = 20 °C. Compared with Fig. 10 the data for the mixture show enhanced het transfer as expected since vigouros spinodal decomposition does occur for T_{Cu} = 20 °C.

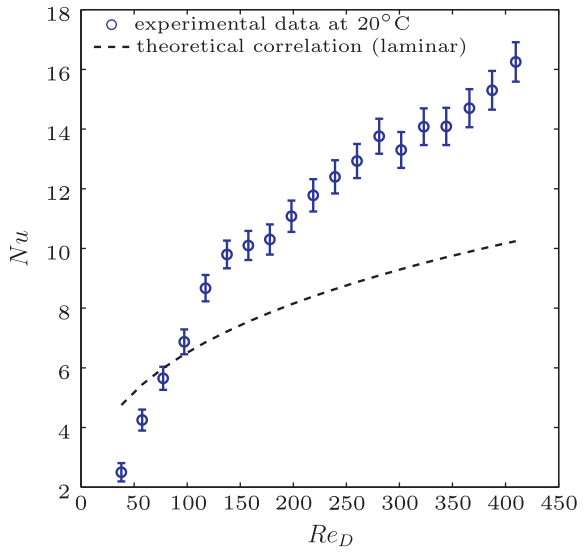

Fig. 11. Comparison between theoretical and experimental Nusselt numbers in a single-channel with a critical mixture of acetone and hexadecane, T_{bath} = 35 °C and T_{Cu} = 20 °C. Here the quench is deep enough that spinodal decomposition induces a heat transfer enhancement, except for the first five experimental point at low flow rates (that we report for completeness, but may be affected by large errors, see Section 5.2).

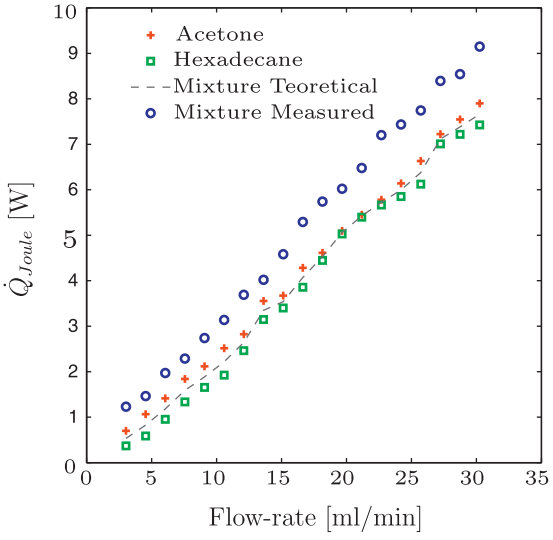

Fig. 13. Electric power absorbed by the parallel heat exchanger with T_{bath} = 35 °C and T_{Cu} = 25 °C, 2 °C quench mild decomposition.

because neither laminar nor turbulent correlations seem to properly predict the Nusselt number.

The first main result for this test section is presented in Fig. 10, where we plot the electrical power absorbed by the resistor during a test made with all our fluids with fixed values of T_{bath} = 35 °C and T_{Cu} = 25 °C. These results are interesting because during this test the bulk temperature does not go below the UCST value of 27 °C in the channel, so there is no decomposition (except a small region near the walls); without decomposition the properties of the mixture are ideally related only to the properties of its constituents. This test demonstrates that the power absorbed with pure acetone, pure hexadecane, and the mixture with critical composition is almost the same.

Then we imposed a lower temperature on the heat exchanger (T_{bath} = 35 °C and T_{Cu} = 20 °C) and we estimated the theoretical Nusselt number for laminar flow using Eq. (4) and assuming that all the mixture thermo-physical properties, except the specific heat, are based on a mass average of the values of the pure fluids. The specific heat of the mixture has been measured with a Differential Scanning Calorimeter and resulted in c_p = 2230 J/(kg K). Fig. 11 shows that the experimental Nusselt number is almost a factor of 2 higher than the theoretical correlation would predict. We take this as a demonstration of the enhancement due to micro-agitation induced by spinodal decomposition.

This is the second main result with the single channel test section. Similarly to Figs. 10 and 12 shows the measured value of $\dot{Q}_{Joule}$

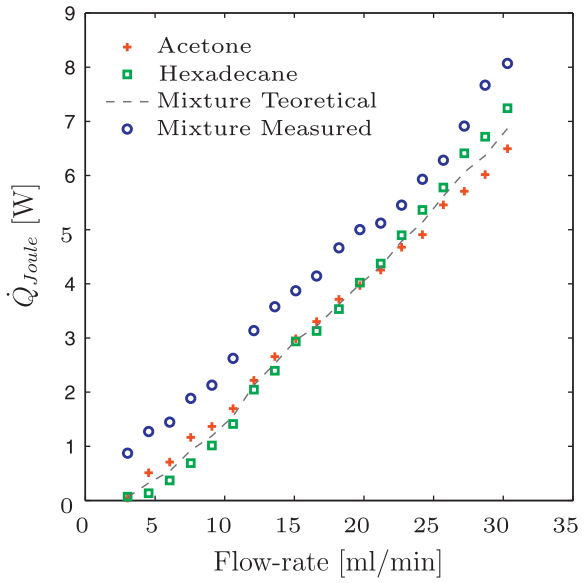

Fig. 14. Electric power absorbed for the U-shape heat exchanger with T_{bath} = 35 °C and T_{Cu} = 25 °C, 2 °C quench mild decomposition.

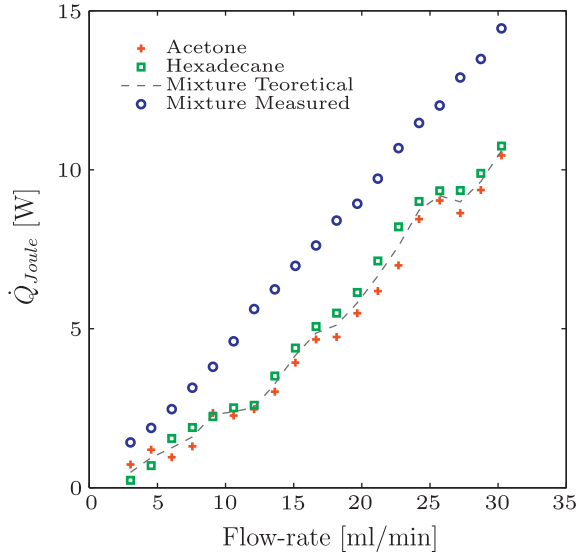

Fig. 15. Electric power absorbed by the parallel heat exchanger with T_{bath} = 35 °C and T_{Cu} = 20 °C, 7 °C quench vigorous decomposition.

versus the flow rate obtained with T_{bath} = 35 °C and T_{Cu} = 20 °C for pure acetone, pure hexadecane, and the critical mixture.

6.2. Multi-channel heat exchangers

As for the single channel, we tested the multichannel exchangers with the same two quench temperatures of 25 °C and 20 °C. With 25 °C, our visualization, shows a mild spinodal decomposition; with 20 °C, instead, the quench is deep enough that we do observe vigorous spinodal decomposition in the section. Figs. 13–16 show the heat exchanged by the pure fluids and the critical mixture.

To evaluate the enhancement effect, we compute the augmentation factor defined as follows:

$$\mathrm{AF} = \frac{\dot{Q}^{\leftarrow}_{\mathrm{Joule}} - \dot{Q}^{\leftarrow}_{\mathrm{Joule}}\big|^{\text{mix without}}_{\text{decomposition}}}{\dot{Q}^{\leftarrow}_{\mathrm{Joule}}\big|^{\text{mix without}}_{\text{decomposition}}} \tag{5}$$

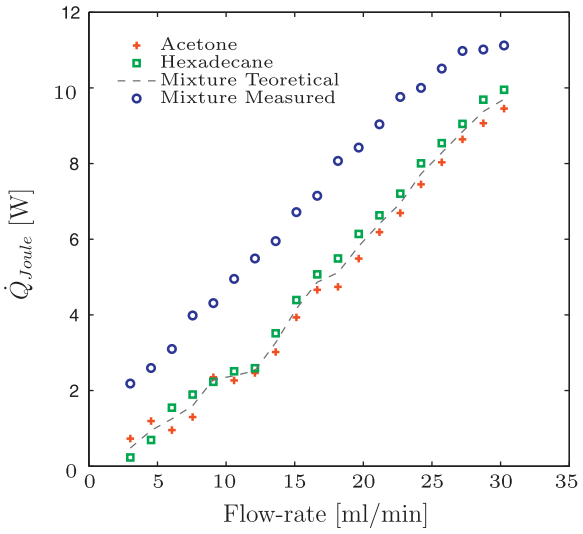

Fig. 16. Electric power absorbed for the U-shape heat exchanger with T_{bath} = 35 °C and T_{Cu} = 20 °C, 7 °C quench vigorous decomposition.

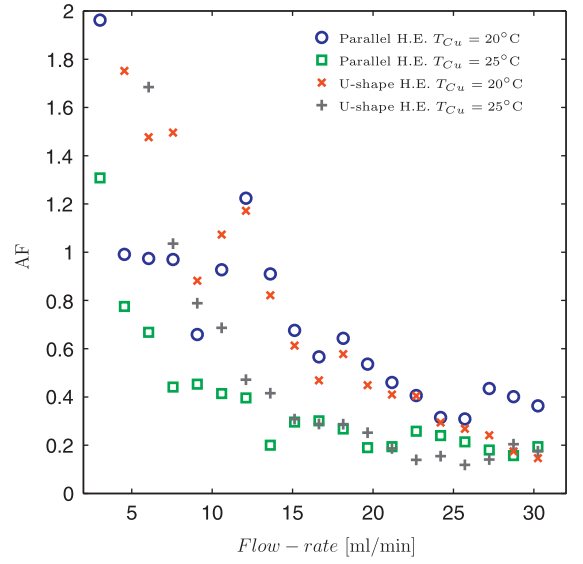

Fig. 17. Heat-transfer Augmentation Factor (AF) as defined by (5), computed from the data in Figs. 13–16.

where $\dot{Q}^{\leftarrow}_{\mathrm{joule}}$ is the measured electrical power absorbed by the hot-reservoir resistor for the actual flow conditions, and $\dot{Q}^{\leftarrow}_{\mathrm{joule}}\big|^{\text{mix without}}_{\text{decomposition}}$ is assumed to be equal to the average of $\dot{Q}^{\leftarrow}_{\mathrm{joule}}\big|_{\text{pure acetone}}$ and $\dot{Q}^{\leftarrow}_{\mathrm{Joule}}\big|_{\text{pure hexadecane}}$ measured at the same flow rate. This assumption is justified by the data of Fig. 10 which show that in absence of decomposition the mixture and the two pure components yield approximately the same $\dot{Q}^{\leftarrow}_{\mathrm{joule}}$ for the same flow rate.

Fig. 17 is made using the data of Figs. 13–16. It shows that the performance increase is greater at lower flow rate. This is because there is a sort of summation of the effects: the more is the heat exchanged because of the increase of flow rate the less is the heat exchanged due to the spinodal decomposition induced convection.

The augmentation factor is higher in the multi-channel heat exchangers. This is due to the fact that the tests were conducted under the same flow rates in the two cases, but in the multi channel heat exchangers the flow rate in every single channel is less than the nominal one. Therefore the fluid velocity is smaller and the effect of the induced convection is greater.

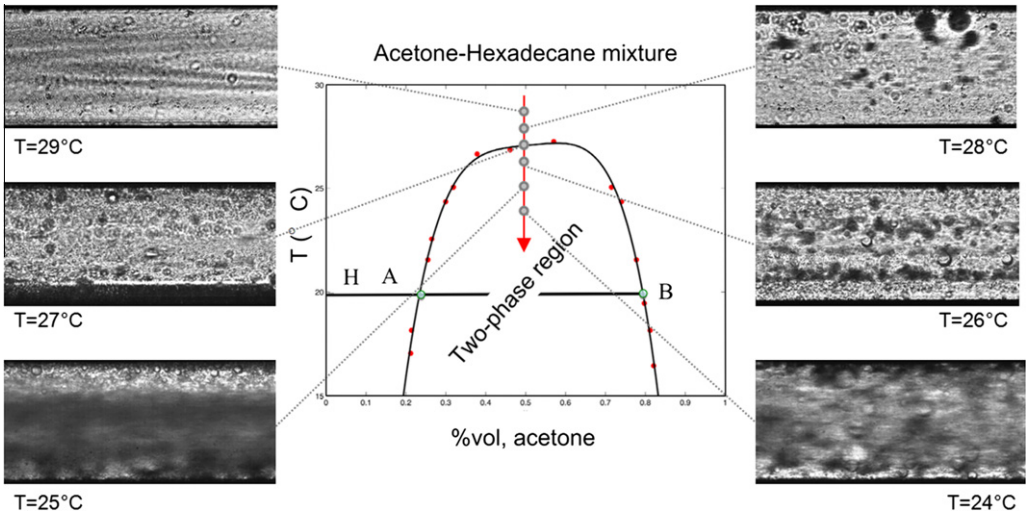

Fig. 18. Effect of quench depth on the vigorousness of the spinodal decomposition of an acetone–hexadecane mixture in a single-channel flow.

6.3. Spinodal decomposition visualization

Comparing Fig. 13 with Figs. 15 and 14 with Fig. 16 shows that the enhancement effect is higher for the deep quench (7 °C in Figs. 15 and 16, 2 °C in Figs. 13 and 14). This is also confirmed by visualizations in single channel setup.

Fig. 18 represents the same piece of channel with constant flow rate (flow rate was set to the lower value possible for our set-up – 1.5 ml/min – to take better pictures) at different T_{Cu} temperatures. We can see that there are two types of flow. At higher temperatures (above the spinodal region) we see the presence of relatively large bubbles; these are probably due to the fact that a little decomposition can be induced by shear in the pipe. At lower temperatures (under the spinodal curve) there is the formation *in situ* of a large number of microdroplets that induce convective motion because of the difference in composition of the two phases. Both effects increase the heat transfer, but the second in much more vigorous way.

7. Conclusions

In this paper we report experimental data on heat transfer enhancement due to spinodal decomposition in single and multi channel heat exchangers. The values of the simplified augmentation factor defined here are higher than those presented in Di Fede et al. [13] ($AF_{id} \approx 0.2$–0.4) obtained with a larger heat exchanger, but lower than those presented in Poesio et al. [11] ($AF_{id} \approx 10$) obtained with fluid at rest). The behavior of our AF seems to follow exactly the trend outlined in these previous papers and support our conclusion that, as expected, the augmentation factor increases as the size of the channels and the flow rate are decreased. From the point of view of applications, this is an important conclusion because small sizes and low flow rates are typically characterized by small Nu numbers and can therefore benefit most from the spinodal enhancement effect.

In the future we are going to decrease as much as possible the size of the channel to obtain higher enhancement factors. Decomposition under temperature gradient is going to be studied too, because we think that the induced convection effect may be amplified by faster coalescence when the spinodal decomposition occurs in a temperature gradient.

Acknowledgements

Work done under AOARD Grant 104146, the Cariplo–UniBS–MIT-MechE faculty exchange program co-sponsored by Università di Brescia and the CARIPLO Foundation, Italy under Grant 2008-2290, and PRIN09 "Studio sperimentale e teorico di aspetti fondamentali del miscelamento liquido-liquido".

References

[1] D.B. Tuckerman, R.F.W. Pease, High-performance heat sinking for VLSI, IEEE Electron Dev. Lett. EDL 2 (5) (1981) 126–129.
[2] H.R. Upadhye, S.G. Kandlikar, Optimization of microchannel geometry for direct chip cooling using single phase heat transfer, in: Proceedings of the Second International Conference on Microchannels and Minichannels (ICMM2004), vol. 679, 2004.
[3] R.K. Shah, A.L. London, Laminar Flow Forced Convection in Ducts: A Source Book for Compact Heat Exchanger Analytical Data, Academic Press, New York, 1978.
[4] I. Mudawar, M.B. Bowers, Ultra-high critical heat flux (CHF) for subcooled water flow boiling-I: CHF data and parametric effects for small diameter tubes, Int. J. Heat Mass Transfer 42 (1999) 1405–1428.
[5] I. Mudawar, Assessment of high-heat-flux thermal management schemes, IEEE Trans. Compon. Pack. Schemes 24 (2001) 122–141.
[6] S. Kandlikar, High heat flux removal with microchannels a roadmap of challenges and opportunities, Heat Transfer Eng. 26 (2005) 59–68.
[7] S.G. Kandlikar, Fundamental issues related to flow boiling in minichannels and microchannels, Exp. Therm. Fluid Sci. 26 (2002) 389–407.
[8] E.N. Wang, L. Zhang, L. Jiang, J. Koo, J.G. Maveety, E.A. Sanchez, K.E. Goodson, Micromachined jets for liquid impingement cooling of VLSI chips, J. Microelectromech. Syst. 13 (2004) 833–842.
[9] A.R. Betz, D. Attinger, Can segmented flow enhance heat transfer in microchannel heat sinks?, Int J. Heat Mass Transfer 53 (2010) 3683–3691.
[10] P. Poesio, G.P. Beretta, T. Thorsen, Dissolution of a liquid microdroplet in a nonideal liquid–liquid mixture far from thermodynamic equilibrium, Phys. Rev. Lett. 103 (2009) 06450.
[11] P. Poesio, A.M. Lezzi, G.P. Beretta, Evidence of heat transfer enhancement induced by spinodal decomposition, Phys. Rev. E 75 (2007) 066306.
[12] S. Gat, N. Brauner, A. Ullmann, Heat transfer enhancement via liquid–liquid phase separation, Int. J. Heat Mass Transfer 52 (2009) 1385–1399.
[13] F. Di Fede, P. Poesio, G.P. Beretta, Heat transfer enhancement in a mini-channel by liquid–liquid spinodal decomposition, Int. J. Heat Mass Transfer (2011).
[14] D. Molin, R. Mauri, Enhanced heat transport during phase separation of liquid binary mixtures, Phys. Fluids 19 (2007) 074102.
[15] E. Machedo, P. Rasmussen, Liquid–liquid equilibrium data collection, DeChema Data Ser. V (part 4, 52) (1987).
[16] K. Stephan, P. Preuer, Wärmeübergang und maximale Wärmestromdichte beim Behältersieden binärer und ternärer Flüssigkeitsgemisch, Chem. Ing. Tech. 51 (1979) 37.
[17] V. Gnielinski, New equations for heat and mass-transfer in turbulent pipe and channel flow, Int. Chem. Eng. 16 (1976) 359–368.